Subgigahertz-resolution table-top spectrograph calibrated with a 4-GHz optical frequency comb

Mamoru Endo
Takashi Sukegawa
Alissa Silva
Yohei Kobayashi

Subgigahertz-resolution table-top spectrograph calibrated with a 4-GHz optical frequency comb

Mamoru Endo,[a,b] Takashi Sukegawa,[c] Alissa Silva,[a,b] and Yohei Kobayashi[a,b,*]

[a]The University of Tokyo, The Institute for Solid State Physics, Kashiwa, Japan
[b]Japan Science and Technology Agency, Exploratory Research for Advanced Technology, Tokyo, Japan
[c]Canon Inc., Optical Products Operations, Utsunomiya, Japan

Abstract. We developed a table-top multipass spectrograph with a 610-MHz resolution (corresponding to a resolving power of 450,000) and a throughput of 10%. The spectrograph was calibrated with a 4-GHz optical frequency comb (OFC) that did not require filtering cavities, which would hinder long-term operation. The OFC is centered at a wavelength of 1 μm, which makes it suitable for the investigation of M dwarf stars and the compact size of the OFC-calibrated spectrograph makes it suitable for use in small to mid-scale observatories.

1 Introduction

In recent years, calibration methods of astronomical spectrographs using optical frequency combs (OFCs)[1] with repetition rates exceeding 10 GHz have been successfully developed.[2,3] An OFC generates equally spaced longitudinal modes, ν_n ($\nu_n = f_0 + n f_{\rm rep}$, where f_0 is the carrier-envelope offset frequency and $f_{\rm rep}$ is the repetition rate) within a broad spectrum, and the optical frequency of each longitudinal mode can be precisely determined via a radio frequency (rf) or an optical frequency standard. In addition to these properties, using an OFC as a frequency calibration source for spectrographs has the following advantages: the ability to calibrate detectors that present nonlinearities such as charge-coupled devices (CCDs), the traceability to fundamental constants such as rubidium (Rb) or cesium (Cs) atomic clocks, and the capacity to generate a wideband spectrum typically spanning the bandwidth of the spectrograph. These advantages have enabled the measurement of Doppler wavelength shifts induced by the radial velocity (RV) of stars, i.e., their motion, to an accuracy of several cm/s.[3–6] At such accuracy levels, the minute Doppler shifts stemming from orbiting Earth-analog planets can be detected. OFCs are expected to replace Th–Ar lamps or I_2 cells, which have been widely used as calibration sources so far.

Most OFCs used for astronomical spectroscopy emit in the visible.[2,3] However, OFCs with a near-infrared (NIR) spectrum are ideal candidates for the detection of Earth-like planets orbiting M dwarf stars as the latter have a spectral energy distribution peak in the NIR.[7] M dwarf stars have relatively low temperatures and their emission spectrum is centered in the NIR (900 to 1800 nm). M dwarf stars have close-in habitable zones[8] due to their low mass and cool temperatures, and Earth-analog planets in this zone affect the larger RV shift of the star's spectrum. Typically, this RV value for M dwarf stars is in the order of 1 m/s, which is ten times higher than that of the RV shift of the Sun with its Earth-analog planets. The study and detection of M dwarf stars and their exoplanets is of great interest as they make up 70% of the stars within 10 parsec of

---

*Address all correspondence to Yohei Kobayashi, E-mail: yohei@issp.u-tokyo.ac.jp

the Earth.[9–11] NIR RV measurements are, however, limited by the availability of suitable NIR sources to precisely calibrate spectrographs. Although lamps and gas cells have been used as calibration sources in the NIR,[12,13] they offer few and unequally spaced lines of unstable intensity. On the other hand, NIR OFCs offer equally spaced lines of stable intensity and they have demonstrated the measurement of RVs with accuracy levels of several m/s.[10]

Despite such advantages, some aspects of OFC-calibrated spectrographs remain to be improved, namely the technical challenges detailed below and the fact that only a few large-scale observatories can install them. The search for exoplanets requires long-running measurements, typically lasting several months or years, and it is difficult to schedule periods of sufficiently long times to carry them out in large-scale observatories. It is preferable to undertake these experiments in smaller scale observatories, however, therein lie two technical challenges, one has to do with the OFC and the other has to do with the spectrometer. Where the OFC is concerned, the obstacle comes from the repetition rate being typically limited to <1 GHz. As the resolution of astronomical spectrometers is limited to several GHz, an OFC with a similar mode spacing is desirable. To achieve this, several stages of filtering cavities and optical amplifiers are typically used.[14] However, cavities with multistage filters reduce the long-term stability of OFCs, they add complexity to their operation, and their instability is increased as a result of super-mode noise, where after amplification, noise grows to the extent of preventing efficient calibration of spectrographs.[6,15] Octave-spanning GHz OFCs are also an option, however, broadening their spectra is a challenge due to their low pulse energies. It is worth noting, however, that recent progress with highly nonlinear media, such as photonic crystal fibers (PCFs), highly nonlinear fibers (HNLFs), and Si_3N_4 waveguides, have led to the generation of octave-spanning spectra, even with pulse energies as low as sub-nJ.[16–18] The technology of several-hundred MHz repetition rate OFCs is sufficiently advanced so that ultra-low phase noise MHz OFCs are widely and commercially available and when ultra-low phase noise operation is not required, phase-locking an OFC to another, such as a GHz OFC to a MHz OFC, is a common enough technique, which makes our developed method a suitable turn-key solution for the calibration of astronomical spectrographs.

Where the spectrometer is concerned, the challenge lies in the generation of a spectrum with a sufficiently high signal-to-noise-ratio (SNR). A spectrometer that offers both a high resolution and a high SNR would circumvent the need for a high-repetition-rate OFC and a typical one with a lower repetition rate could be used without the assistance of filtering cavities.

In this letter, we present the development of an NIR 4-GHz repetition-rate OFC that does not use filtering cavities and that is employed for the calibration of a sub-GHz resolution spectrometer in a multipass configuration. A 610-MHz frequency resolution spectrograph ($R = f/\Delta f = 450,000$) was obtained with a seven-pass configuration, and each longitudinal mode of the 4-GHz OFC was clearly resolved. This spectrograph is based on a single-mode fiber arrangement and is not diffraction-limited (unlike that in Ref. 19), as it suffers from astigmatism. Typically, coupling light from a telescope into a fiber is challenging, however, recently engineered adaptive-optics technology might help improve the coupling efficiency.[20,21] We believe that the experimental OFC-calibrated spectrograph, as detailed in this letter, is simple and could be easily implemented in relatively small to mid-scale observatories.

The concept of this method, as reported in the conference proceedings article,[22] was modified to improve the linewidth of the comb modes from 500 kHz down to <1 Hz, which helped to achieve a significantly more precise calibration of the spectrograph via altering the optical phase-locking of the OFC.

2 Experiments

2.1 *4-GHz Optical Frequency Comb*
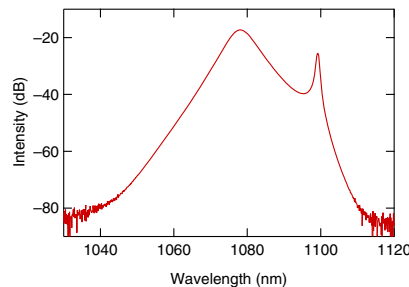
Figure 1 shows a schematic diagram of the 4-GHz OFC configuration, the highlight of which is the Yb:Y_2O_3 ceramic Kerr-lens mode-locked laser. The laser configuration follows that of our previously developed 6-GHz Yb:Lu_2O_3 ceramic laser.[23] The resonator is a bow-tie ring cavity with two concave mirrors ($r = 15$ mm) and two plane mirrors, and the net cavity length was set
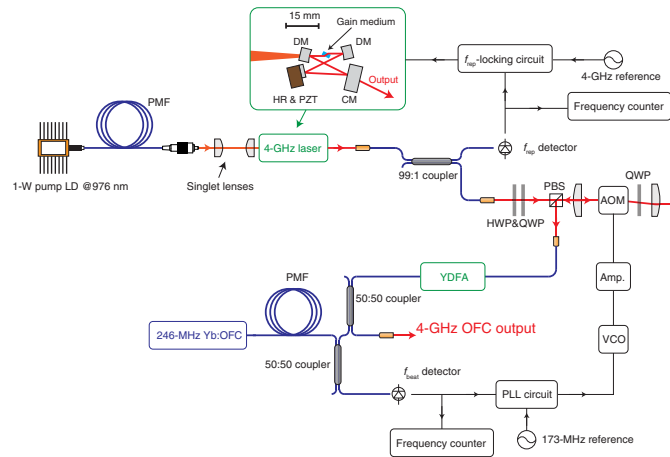
Fig. 1 The experimental apparatus of the 4-GHz OFC. PMF, polarization-maintaining fiber; DM, dichroic mirror; HR, high-reflection mirror; CM, chirped-coated mirror; HWP (QWP), half (quarter)-wave plate; gain medium, 2-mm-thick; noncoated 3 at. % $Yb:Y_2O_3$ ceramic; PBS, polarization beam splitter; VCO, voltage-controlled oscillator; Amp., RF amplifier; f_{rep} (f_{beat}) detector: 25-GHz (2-GHz) InGaAs photodetector; and YDFA, Yb-doped fiber amplifier.

to 46 mm. Both concave mirrors were dichroic mirrors (DMs) coated for high reflection (HR) at 1080 nm and high transmission at 976 nm. The plane mirrors were both HR-coated for 1080 nm. One of them was mounted on a piezoelectric actuator to allow phase stabilization of the repetition rate, whereas the other was chosen to be a chirped mirror (CM) to compensate the intracavity dispersion. The total group delay dispersion of the oscillator was estimated to be -100 fs^2, which allowed sufficiently high peak powers to induce the Kerr-lens effect. The gain medium, a 2-mm-thick noncoated 3 at. % $Yb:Y_2O_3$ ceramic, was mounted on a copper plate and placed between the two concave mirrors at the Brewster angle. The ceramic gain medium was pumped by a single-mode-fiber coupled fiber-Bragg-grating stabilized 976-nm laser diode with a maximum power of 1 W. The folding angles at the concave mirrors were adjusted to 11 deg to compensate the astigmatism caused by the Brewster-placed ceramic. The pump beam was collimated then focused down to the center of the ceramic by a pair of singlet lenses ($f = 25$ and 40 mm, respectively). The CM had a transmittance of 0.04% and was used as the output coupler. After optimization of the cavity alignment for continuous-wave (cw) operation, by adjusting the position of one of the concave mirrors, stable Kerr-lens mode-locked operation was obtained. In the ring cavity, both clockwise and counterclockwise oscillations were possible for cw operation, and two output beams were observed from the output coupler. When the laser was mode-locked, one of the output beams disappeared and the output power in the other would increase, indicating that a single oscillation direction was permitted inside the cavity for mode-locked operation. Under the mode-locked condition, the pulse spectrum was centered at a wavelength of 1078 nm with a FWHM of 7 nm and the Fourier transform-limited pulse duration was 174 fs. The optical spectrum is shown in Fig. 2. When the pump power was 700 mW, an output power of 20 mW was obtained and stable mode-locking was maintained for several days. The stabilization

Fig. 2 The optical spectrum of the 4-GHz OFC. The spectrum width was 7 nm at the center wavelength of 1078 nm.
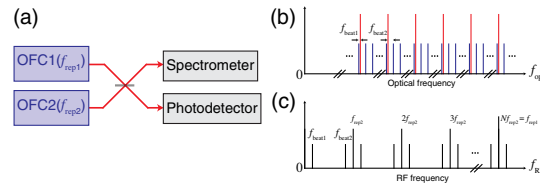
Fig. 3 Beat signals between two OFCs with different repetition rates of f_{rep1} and f_{rep2}. (a) A simplified schematic diagram of the experiment, where OFC1 is the 4-GHz comb and OFC2 is the 250-MHz one. (b) Optical frequency domain representation of a spectrum, as would be measured by an optical spectrum analyzer, of the interference between the modes of the 4-GHz OFC and 250-MHz OFC. (c) Is the same as (b), only it is the rf domain representation of a spectrum as would be measured by an electronic spectrum analyzer.

of each single mode of a frequency comb was achieved via phase-locking both the carrier-envelope offset (f_0) and repetition frequencies (f_{rep}). Typically, in the case of the carrier-envelope offset frequency, phase-locking is achieved via the self-referencing technique, which consists in part of generating an octave-spanning spectrum using a highly nonlinear fiber. However, repetition rates as high as 4 GHz prevent such spectral broadening, therefore, stabilization was carried out by phase-locking the comb modes to those of a 250-MHz Yb-fiber OFC whose repetition rate was one sixteenth that of 4 GHz. Both repetition frequencies were phase-locked to rf standards, thus keeping the frequency ratio of 16:1, and in this way, the observed beat signal between the 250-MHz OFC and the 4-GHz oscillator would correspond to the difference between the carrier-envelope offset frequencies as shown in Fig. 3. To achieve this, the beams from the two OFCs were coupled into a 50:50-fiber combiner, and the beat signal was detected at the f_{beat} detector. When the repetition rate of the 250-MHz OFC was one-Nth ($N = 16$ in our experiment) of the 4-GHz OFC repetition rate, the beat signals between all modes of the two OFCs were the same over the entire overlapping region of the combs' spectra.

The 4-GHz repetition frequency was locked to a Rb-clock referenced rf standard using a 25-GHz-bandwidth InGaAs detector (f_{rep} detector) and an analogue locking circuit. An acousto-optic modulator (AOM) and a phase-locked-loop circuit were used to phase-lock the beat signal to the reference frequency (chosen here as 173 MHz). The AOM was mounted in a double-pass configuration to avoid shifts in the beam pointing when the frequency was tuned. An Yb-doped fiber amplifier (YDFA) was placed after the AOM to increase the SNR of the beat signal for efficient detection. The output power as measured at "4-GHz OFC output" in Fig. 1 was ~50 mW.

Figure 4 shows the beat signal when the 4-GHz frequency comb was free-running (a) and when it was phase-locked (b). Although the locking bandwidth was limited to ~100 kHz by the modulation bandwidth of the voltage-controlled oscillator (VCO) used with the AOM, a higher bandwidth (over a MHz) could be obtained by simply replacing the VCO with one that has a higher modulation bandwidth. Higher phase-locking bandwidths and higher amplitudes of the frequency modulation are required for frequency combs with GHz repetition rates over those with sub-GHz repetition rates, since cavity length fluctuations result in larger frequency shifts of the comb modes. In order to maintain the phase-locking of the repetition rate for a longer time
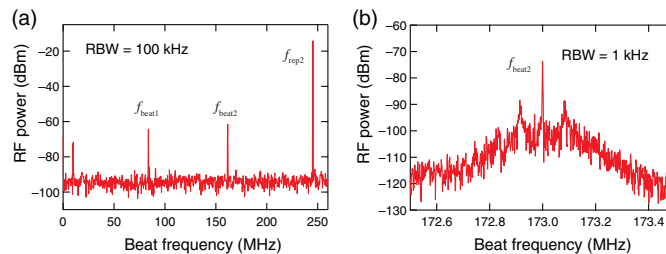

Fig. 4 Spectra of beat signals measured with f_{beat} detector. (a) Free-running signal measured with a resolving bandwidth (RBW) of 100 kHz. (b) Phase-locked beat signal acquired with an RBW of 1 kHz.

still, the oscillator could be temperature controlled, however, this was not done here. The modulation bandwidth and the fact the cavity was not temperature controlled restricted the long-term and phase stabilities of the system, but under the standard laboratory conditions, the OFC was stable over multiple days without the need for any stabilization.

2.2 Multipass Spectrograph with a Frequency Resolution of Sub-GHz

A multipass spectrograph, as depicted in Fig. 5(a), was assembled using a transmission grating (1740 g/mm) with a high efficiency (90% at $\lambda = 1080$ nm) and a large size (180 mm × 40 mm). The transmission grating (made by Canon Inc.) was fabricated by optical lithography means and further details can be found in Ref. 24. Owed to the multipass configuration, the spectrometer had a relatively small footprint (~0.5 m × 1 m). The stabilized output of the 4-GHz frequency comb was guided to the spectrograph configuration via a polarization-maintaining single-mode fiber (PMF), the core of which (6 μm mode-field diameter) served as an incident slit for the spectrometer. The light was collimated to a line shape (~1 mm × 25 mm) by two perpendicularly placed cylindrical lenses [with focal lengths of 15 mm (CYL 1, LJ1636L2-B, Thorlabs) and 150 mm (CYL 2, ACY254-150-B, Thorlabs), respectively]. The light incident on the grating was diffracted multiple times using mirrors (HR 1, 2, and 3) until the desired resolution was obtained. Figures 5(b) and 5(c) illustrate the beam path of a simple three-pass configuration. In our experiments, the number of diffractions was extended to 7 with this same configuration. The numbers (1 to 6) point to the order in which the beam is being diffracted or reflected after collimation at CYL 2. The line-shaped light from CYL 2 was first diffracted by the grating (1), then reflected by HR 2 (2). The light was diffracted again at the grating (3). The mirror HR 1 was slightly tilted in the vertical direction, so that after the second diffraction at point (3), the beam was ~1 mm below the first one (1). The diffracted light was reflected at HR 2 (4); then diffracted at (5). In Figs. 5(b) and 5(c), the three-times diffracted light was reflected off of HR 3 (6) and directed toward CYL 3. The multiply diffracted light was then focused onto a CCD camera (3312 × 2488 pixels, 14-bit resolution, IGV B3320M, IMPERX) by two perpendicularly placed cylindrical lenses [with focal lengths of 500 mm (CYL 3, specially designed by
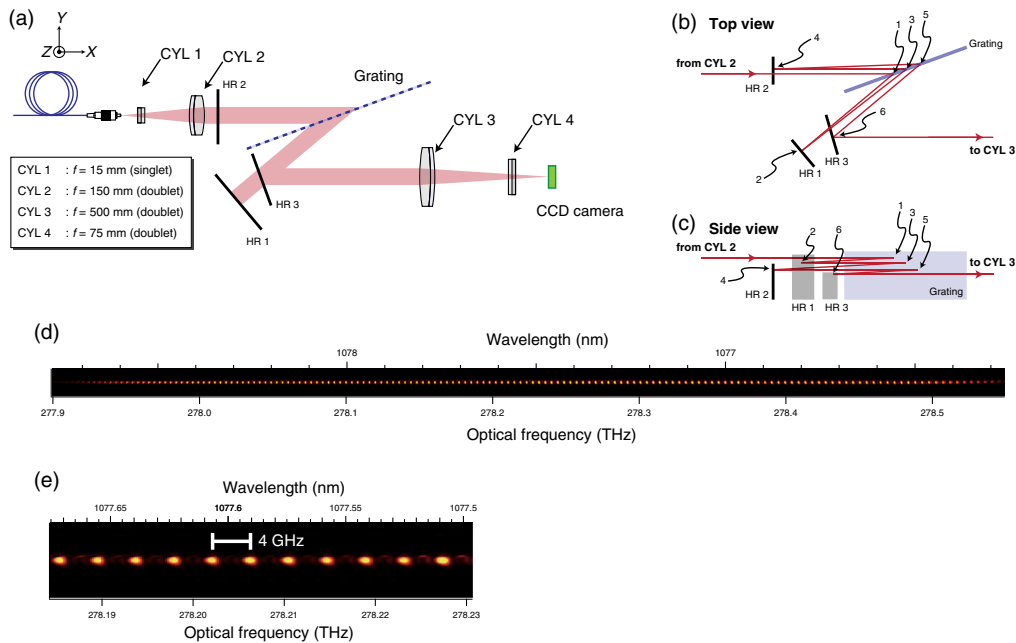
Fig. 5 (a)–(c) The experimental configuration of the multipass spectrometer. (b), (c) The top and side views, respectively, of the beam path. The beam was diffracted or reflected from 1 to 6 at the grating or the high-reflection mirrors (HR 1, 2, and 3). In this figure, the beam was diffracted 3 times at the grating. (d), (e) The resolved comb modes of the 4-GHz OFC by the multipass spectrograph when the center wavelength was set to 1077.5 nm. (e) The expanded image.

Table 1 Number of diffractions and corresponding measured resolution.

Number of diffractions	Resolution (MHz)	Resolving power ($f/\Delta f$)
3	1500	180,000
5	790	350,000
7	610	450,000

OptoSigma) and 75 mm (CYL 4, ACY254-075-B, Thorlabs), respectively]. To reduce aberrations, three of the cylindrical lenses used were doublets (achromatic lenses). Upon the CCD surface, the diameter of the focused beam was 25 μm and the beam spot separation was 150 μm for a seven-pass configuration. With this configuration, a 610-MHz frequency resolution was calculated ($R = f/\Delta f = 450,000$), and each longitudinal mode of the 4-GHz OFC was clearly resolved at the CCD camera, as shown in Figs. 5(d) and 5(e). The presence of weak beam spots in between each main one was most likely due to aberrations of the achromatic cylindrical lenses. Typically, the assembly of an achromatic cylindrical lens is harder than that of a standard achromatic one, as they are more sensitive to the axis of alignment. Since the size of the collimating and focusing lenses used was limited, diffraction effects occurred at these lenses. These aberrations and diffraction effects contributed to a focal spot size that is slightly larger than the anticipated diffraction-limited one of ~20 μm. Lenses with larger diameters could help reduce these effects and improve the frequency resolution.

The spectrometer had a bandwidth of 1 nm centered at the wavelength of 1077.5 nm and a throughput of over 10% was achieved with the resolution of 610 MHz. The center wavelength could be changed by rotating the grating and HR 1. The frequency resolutions and resolving powers are detailed in Table 1. Although the setup described in Fig. 5 enabled the use of light having undergone an odd number of diffractions, an even number of diffractions was achieved by simply changing the spectrograph configuration.

3 Conclusions

In this paper, we present the development of a 4-GHz OFC and a compact 610-MHz resolution spectrograph in a multipass configuration. The optical frequencies of the comb modes were stabilized to a 250-MHz Yb-fiber OFC, which itself was phase locked to a Rb standard. The longitudinal modes of the 4-GHz OFC were clearly resolved thanks to its high repetition rate and the high resolution of the spectrometer. A large-sized transmission grating enabled the assembly of a high-resolution spectrograph with a simple and compact configuration. We believe many observatories could simply install similar OFC-calibrated spectrographs.

Acknowledgments

References

1. S. T. Cundiff and J. Ye, "Colloquium: femtosecond optical frequency combs," *Rev. Mod. Phys.* **75**(1), 325–342 (2003).
2. T. Steinmetz et al., "Laser frequency combs for astronomical observations," *Science* **321**(5894), 1335–1337 (2008).
3. T. Wilken et al., "A spectrograph for exoplanet observations calibrated at the centimetre-per-second level," *Nature* **485**(7400), 611–614 (2012).

4. C. H. Li et al., "A laser frequency comb that enables radial velocity measurements with a precision of 1 cm s^{-1}," *Nature* **452**(7187), 610–612 (2008).

5. A. G. Glenday et al., "Operation of a broadband visible-wavelength astro-comb with a high-resolution astrophysical spectrograph," *Optica* **2**(3), 250 (2015).

6. R. A. McCracken, J. M. Charsley, and D. T. Reid, "A decade of astrocombs: recent advances in frequency combs for astronomy [Invited]," *Opt. Express* **25**, 15058 (2017).

7. A. Reiners et al., "Detecting planets around very low mass stars with the radial velocity method," *Astrophys. J.* **710**(1), 432–443 (2010).

8. R. K. Kopparapu et al., "Habitable zones around main-sequence stars: new estimates," *Astrophys. J.* **765**(2), 131 (2013).

9. G. G. Ycas et al., "Demonstration of on-sky calibration of astronomical spectra using a 25 GHz near-IR laser frequency comb," *Opt. Express* **20**(6), 6631 (2012).

10. A. J. Metcalf et al., "Stellar spectroscopy in the near-infrared with a laser frequency comb," *Optica* **6**(2), 233 (2019).

11. T. Henry et al., "The solar neighborhood. XVII. parallax results from the CTIOPI 0.9 m program: 20 new members of the RECONS 10 parsec sample," *Astron. J.* **132**(6), 2360–2371 (2006).

12. S. L. Redman et al., "The infrared spectrum of uranium hollow cathode lamps from 850 nm to 4000 nm: wavenumbers and line identifications from Fourier transform spectra," *Astrophys. J. Suppl. Ser.* **195**(2), 24 (2011).

13. S. Mahadevan and J. Ge, "The use of absorption cells as a wavelength reference for precision radial velocity measurements in the near-infrared," *Astrophys. J.* **692**(2), 1590–1596 (2009).

14. F. Quinlan et al., "A 12.5 GHz-spaced optical frequency comb spanning >400 nm for near-infrared astronomical spectrograph calibration," *Rev. Sci. Instrum.* **81**(6), 063105 (2010).

15. G. Chang et al., "Toward a broadband astro-comb: effects of nonlinear spectral broadening in optical fibers," *Opt. Express* **18**, 12736 (2010).

16. C. Benko et al., "Full phase stabilization of a Yb:fiber femtosecond frequency comb via high-bandwidth transducers," *Opt. Lett.* **37**, 2196 (2012).

17. A. S. Mayer et al., "Frequency comb offset detection using supercontinuum generation in silicon nitride waveguides," *Opt. Express* **23**(12), 15440 (2015).

18. D. R. Carlson et al., "Self-referenced frequency combs using high-efficiency silicon-nitride waveguides," *Opt. Lett.* **42**(12), 2314 (2017).

19. J. R. Crepp et al., "iLocater: a diffraction-limited Doppler spectrometer for the Large Binocular Telescope," *Proc. SPIE* **9908**, 990819 (2016).

20. G. J. Monnet, "Overview of the VLT instrumentation," *Proc. SPIE* **3355**, 2–7 (1998).

21. J. Ge et al., "An optical ultrahigh-resolution cross-dispersed Echelle spectrograph with adaptive optics," *Publ. Astron. Soc. Pac.* **114**(798), 879–891 (2002).

22. M. Endo et al., "Development of compact and ultra-high-resolution spectrograph with multi-GHz optical frequency comb," *Proc. SPIE* **9147**, 91477Y (2014).

23. M. Endo, A. Ozawa, and Y. Kobayashi, "6-GHz, Kerr-lens mode-locked Yb:Lu_2O_3 ceramic laser for comb-resolved broadband spectroscopy," *Opt. Lett.* **38**, 4502 (2013).

24. C. Zhou et al., "Wavefront analysis of high-efficiency, large-scale, thin transmission gratings," *Opt. InfoBase Conf. Pap.* **22**(5), 5995–6008 (2014).